The far-infrared view of M87 as seen by the Herschel Space Observatory

M. Baes[1], M. Clemens[2], E. M. Xilouris[3], J. Fritz[1], W. D. Cotton[4], J. I. Davies[5], G. J. Bendo[6], S. Bianchi[7], L. Cortese[5], I. De Looze[1], M. Pohlen[5], J. Verstappen[1], H. Böhringer[8], D. J. Bomans[9], A. Boselli[10], E. Corbelli[7], A. Dariush[5], S. di Serego Alighieri[7], D. Fadda[11], D. A. Garcia-Appadoo[12], G. Gavazzi[13], C. Giovanardi[7], M. Grossi[14], T. M. Hughes[5], L. K. Hunt[7], A. P. Jones[15], S. Madden[16], D. Pierini[8], S. Sabatini[17], M. W. L. Smith[5], C. Vlahakis[18], S. Zibetti[19]

[1]Sterrenkundig Observatorium, Universiteit Gent, Belgium

[2]INAF-Osservatorio Astronomico di Padova, Italy

[3]National Observatory of Athens, Greece

[4]National Radio Astronomy Observatory, USA

[5]Department of Physics and Astronomy, Cardiff University, UK

[6]Astrophysics Group, Imperial College London, UK

[7]INAF-Osservatorio Astrofisico di Arcetri, Firenze, Italy

[8]Max-Planck-Institut für Extraterrestrische Physik, Garching, Germany

[9]Astronomical Institute, Ruhr-University Bochum, Germany

[10]Laboratoire d'Astrophysique de Marseille, France

[11]NASA Herschel Science Center, California Institute of Technology, USA

[12]European Southern Observatory, Santiago, Chile

[13]Università di Milano-Bicocca, Italy

[14]CAAUL, Observatório Astronómico de Lisboa, Portugal

[15]Institut d'Astrophysique Spatiale (IAS), Université Paris-Sud 11, France

[16]Laboratoire AIM, CEA/DSM, Université Paris Diderot, France

[17]INAF-Istituto di Astrofisica Spaziale e Fisica Cosmica, Roma, Italy

[18]Leiden Observatory, The Netherlands

[19]Max-Planck-Institut für Astronomie, Heidelberg, Germany

Abstract. The origin of the far-infrared emission from the nearby radio galaxy M87 remains a matter of debate. Some studies find evidence of a far-infrared excess due to thermal dust emission, whereas others propose that the far-infrared emission can be explained by synchrotron emission without the need for an additional dust emission component. We observed M87 with PACS and SPIRE as part of the Herschel Virgo Cluster Survey (HeViCS). We compare the new Herschel data with a synchrotron model based on infrared, submm and radio data to investigate the origin of the far-infrared emission. We find that both the integrated SED and the Herschel surface brightness maps are adequately explained by synchrotron emission. At odds with previous claims, we find no evidence of a diffuse dust component in M87.

1. Introduction

At a distance of 16.7 Mpc, M87 is the dominant galaxy of the Virgo Cluster. It is one of the nearest radio galaxies and was the first extragalactic X-ray source to be identified. Because of its proximity, many interesting astrophysical phenomena can be
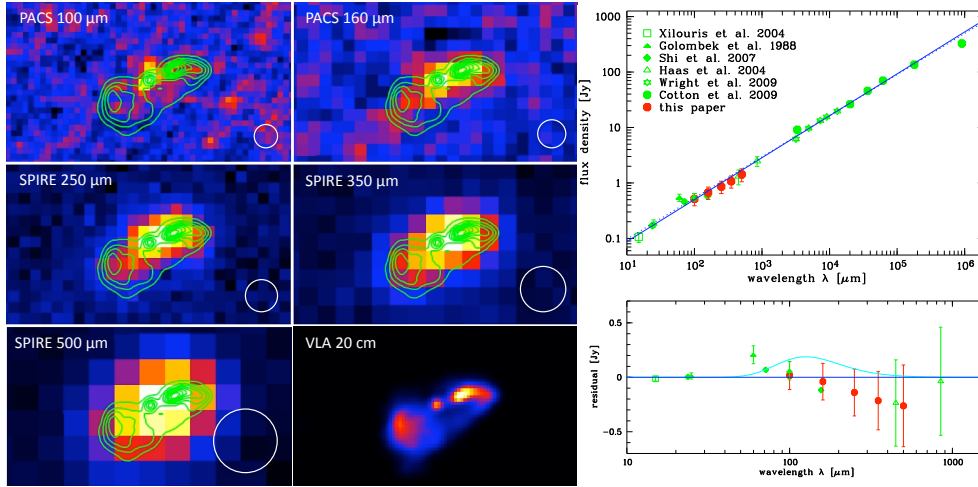
Figure 1. Left: the Herschel view of the central regions of M87. The bottom right image is a VLA 20 cm image from the FIRST survey. The 20 cm radio contours have been overlaid on the Herschel images. The field of view of all images is 160" × 90", beam sizes are indicated in the bottom right corner. Top right: the global SED of M87 from mid-infrared to radio wavelengths. Where no error bars are seen, they are smaller than the symbol size. The solid line in the plot is the best-fit power law of the ISOCAM, IRAS, MIPS, SCUBA, GBT, WMAP, and VLA data; the dotted line has only been fitted to the SCUBA, GBT, WMAP, and VLA data. Bottom right: residual between data and the best-fit synchrotron model in the infrared-submm wavelength range. The cyan line is a modified black-body model with $T = 23$ K and $M_d = 7 \times 10^4$ $M_\odot$.

studied in more detail in M87 than in other comparable objects. Particularly remarkable is the prominent jet extending from the nucleus, visible throughout the electromagnetic spectrum. The central regions of M87, in particular the structure of the jet, have been studied and compared intensively at radio, optical, and X-ray wavelengths. (e.g. Biretta et al. 1991; Meisenheimer et al. 1996; Böhringer et al. 2001; Perlman et al. 2001; Sparks et al. 2004; Perlman & Wilson 2005; Kovalev et al. 2007; Simionescu et al. 2008).

Compared to the available information at these wavelengths, our knowledge of M87 at far-infrared (FIR) wavelengths is rather poor. A controversial issue is the origin of the FIR emission in M87, i.e., the question of whether the FIR emission is caused entirely by synchrotron emission or whether there is an additional contribution from dust associated with either the global interstellar medium or a nuclear dust component. Several papers, based on IRAS, ISO and Spitzer observations, arrive at different conclusions (Perlman et al. 2007; Buson et al. 2009; Xilouris et al. 2004; Shi et al. 2007; Tan et al. 2008).

We investigate the nature of the FIR emission of M87 using new FIR data from the Herschel Space Observatory (Pilbratt et al. 2010), obtained as part of the science demonstration phase (SDP) observations of the Herschel Virgo Cluster Survey (HeViCS, Davies et al. 2010). HeViCS is an approved open time key program, which has been awarded 286 h of observing time in parallel mode with the PACS and SPIRE instruments. We will ultimately map four 4 × 4 square degree regions of the cluster at 100, 160, 250, 350 and 500 μm, down to the 250 μm confusion limit of about 1 MJy sr^{-1}. The HeViCS SDP observations consisted of a single cross-scan of one 4 × 4 deg^2 field at the centre of the Virgo Cluster. While these SDP observations comprise only 6% of the total HeViCS observations, the analysis based on these observations already gives a prelude to the primary HeViCS science goals including the effects of the environment on the dust medium of galaxies, the FIR luminosity function, the complete SEDs of galaxies and a detailed
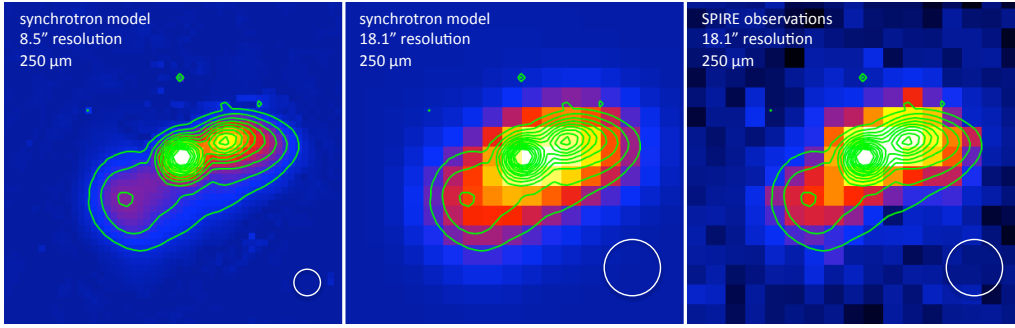
Figure 2. A comparison between the synchrotron model image and the observed image at 250 μm. The left panel shows the synchrotron image at the model resolution, the central panel shows the same model convolved to the SPIRE 250 μm beam and pixel size. The right panel shows the observed SPIRE 250 μm image. In all panels, the green lines are the contours of the synchrotron model at the model resolution.

analysis of the dust content of dwarf and early-type galaxies (Davies et al. 2010; Cortese et al. 2010; Clemens et al. 2010; Smith et al. 2010; Grossi et al. 2010; De Looze et al. 2010; Boselli et al. 2010). The observations also enabled us to study the intensity and nature of the FIR emission of M87 (Baes et al. 2010).

2. Analysis and conclusion

The left part of Figure 1 shows the PACS and SPIRE images of the central 160" × 90" region of M87, which is clearly detected in all five bands. The top right panel in Figure 1 shows the integrated SED in the infrared-submm-radio region between 15 μm and 100 cm, with the new Herschel data as well as ISOCAM, IRAS, MIPS, and SCUBA, GBT, WMAP, and VLA data gathered from the literature (Xilouris et al. 2004; Golombek et al. 1988; Shi et al. 2007; Haas et al. 2004; Cotton et al. 2009; Wright et al. 2009); the actual flux densities can be found in Baes et al. (2010). The solid line is the best-fit power law for all literature data and has a slope $\alpha = -0.76$; the dotted line fits only the submm and radio data and has a slope $\alpha = -0.74$. The bottom right panel in Figure 1 shows the residual from the best-fit power law in the infrared-submm wavelength region; clearly, the integrated Herschel fluxes are in full agreement with synchrotron radiation. The cyan line in this figure is a modified black-body fitted with $T = 23$ K and $M_d = 7 \times 10^4\ M_\odot$. This temperature is the mean dust equilibrium temperature in the interstellar radiation field of M87, determined using the SKIRT radiative transfer code (Baes et al. 2003, 2005) and based on the photometry from Kormendy et al. (2009). The dust mass was adjusted to fit the upper limits of the residuals. It is clear that the SED of M87 is incompatible with dust masses higher than $10^5\ M_\odot$.

Although indicative, the analysis of the integrated SED does not definitively identify the origin of the FIR emission in M87. Approximating the global SED as a single power-law synchrotron model is indeed an oversimplification of the complicated structure of M87. Several studies have shown that M87 contains three distinct regions of significant synchrotron emission, each with their own spectral indices: the nucleus, the jet and associated lobes in the NW region, and the SE lobes (e.g., Biretta et al. 1991; Meisenheimer et al. 1996; Perlman et al. 2001; Shi et al. 2007). We have constructed a synchrotron model for the central regions of M87, based on a newly reduced MIPS 24 μm map and archival MUSTANG 90 GHz and 15, 8.2, 4.9, 1.6, and 0.3 GHz maps (Cotton et al. 2009). We fitted a second-order polynomial synchrotron model to each pixel of the MIPS + radio

data cube and used this synchrotron model to predict the emission of M87 at 250 μm (the SPIRE 250 μm image provides the optimal compromise between S/N and spatial resolution). Figure 2 shows the comparison between the synchrotron model prediction at 250 μm and the SPIRE observations. At the model resolution, the three distinct components are visible, but when we convolve this synchrotron model image with the SPIRE 250 μm beam, the three different components merge into a single extended structure with one elongated peak slightly west of the nucleus. Comparing the central and right panels of Figure 2, we see that the synchrotron model is capable of explaining the observed SPIRE 250 μm image satisfactorily.

We conclude that for both the integrated SED and the SPIRE 250 μm map, we have found that synchrotron emission is an adequate explanation of the FIR emission. We do not detect a FIR excess that cannot be explained by the synchrotron model. In particular, we have no reason to invoke the presence of smooth dust emission associated with the galaxy interstellar medium, as advocated by Shi et al. (2007). For a dust temperature of 23 K, which is the expected equilibrium temperature in the interstellar radiation field of M87, we find an upper limit to the dust mass of 7×10^4 $M_\odot$. Our conclusion is that, seen from the FIR point of view, M87 is a passive object with a central radio source emitting synchrotron emission, without a substantial diffuse dust component.

References

Baes, M., et al. 2003, MNRAS, 343, 1081
Baes, M., Dejonghe, H., & Davies, J. I. 2005, AIP Conf. Series, 761, 27
Baes, M., et al. 2010, A&A, 518, L53
Biretta, J. A., Stern, C. P., & Harris, D. E. 1991, AJ, 101, 1632
Böhringer, H., et al. 2001, A&A, 365, L181
Boselli, A., et al. 2010, A&A, 518, L61
Buson, L., et al. 2009, ApJ, 705, 356
Clemens, M. S., et al. 2010, A&A, 518, L50
Cortese, L., et al. 2010, A&A, 518, L49
Cotton, W. D., et al. 2009, ApJ, 701, 1872
Davies, J. I., et al. 2010, A&A, 518, L48
De Looze, I., et al. 2010, A&A, 518, L54
Golombek, D., Miley, G. K., & Neugebauer, G. 1988, AJ, 95, 26
Grossi, M., et al. 2010, A&A, 518, L52
Haas, M., et al. 2004, A&A, 424, 531
Kormendy, J., Fisher, D. B., Cornell, M. E., & Bender, R. 2009, ApJS, 182, 216
Kovalev, Y. Y., et al. 2007, ApJ, 668, L27
Meisenheimer, K., Roeser, H.-J., & Schloetelburg, M. 1996, A&A, 307, 61
Perlman, E. S., et al. 2001, ApJ, 551, 206
Perlman, E. S., & Wilson, A. S. 2005, ApJ, 627, 140
Perlman, E. S., et al. 2007, ApJ, 663, 808
Pilbratt, G. L., et al. 2010, A&A, 518, L1
Shi, Y., et al. 2007, ApJ, 655, 781
Simionescu, A., et al. 2008, A&A, 482, 97
Smith, M. W. L., et al. 2010, A&A, 518, L51
Sparks, W. B., et al. 2004, ApJ, 607, 294
Tan, J. C., Beuther, H., Walter, F., & Blackman, E. G. 2008, ApJ, 689, 775
Xilouris, E. M., et al. 2004, A&A, 416, 41
Wright, E. L., et al. 2009, ApJS, 180, 283